

GraphSPME: Markov Precision Matrix Estimation and Asymptotic Stein-Type Shrinkage

Berent Ånund Strømnes Lunde

Equinor
University of Bergen

Feda Curic

Equinor

Sondre Sortland

Equinor

Abstract

GraphSPME is an open source Python, R and C++ header-only package implementing non-parametric sparse precision matrix estimation along with asymptotic Stein-type shrinkage estimation of the covariance matrix. The user defines a potential neighbourhood structure and provides data that potentially are $p \gg n$. This paper introduces a novel approach for finding the optimal order (that data allows to estimate) of a potential Markov property. The algorithm is implemented in the package, alleviating the problem of users making Markov assumptions and implementing corresponding complex higher-order neighbourhood structures. Estimation is made accurate and stable by simultaneously utilising both Markov properties and Stein-type shrinkage. Asymptotic results on Stein-type shrinkage ensure that non-singular well conditioned matrices are obtained in an automatic manner. Final symmetry conversion creates symmetric positive definite estimates. Furthermore, the estimation routine is made efficient and scalable to very high-dimensional problems ($\approx 10^7$) by utilising the sparse nature of the precision matrix under Markov assumptions. Implementation wise, the sparsity is exploited by employing the sparsity possibilities made available by the **Eigen** C++ linear-algebra library. The package and examples are available at <https://github.com/equinor/GraphSPME>.

Keywords: precision, covariance, graph, estimation, shrinkage, Markov, R, Python, C++.

1. Introduction

Efficient and accurate estimation of high-dimensional dependence structures is of increasing importance in computational statistics. Machine-learning algorithms such as LDA and QDA require the computation of precision matrices of the feature vector (Hastie, Tibshirani, Friedman, and Friedman 2009), mixed-effect generalized linear models allow responses to share information through high-dimensional dependence modelling, see e.g. the **mgcv** package (Wood 2011), similar dependence modelling is employed in packages such as **TMB** (Kristensen, Nielsen, Berg, Skaug, and Bell 2015) and **INLA** (Rue, Martino, and Chopin 2009) for calculating the Laplace approximation when working with random effects. Furthermore, ensemble-type filtering algorithms such as the ensemble Kalman filter (Evensen 1994; Burgers, Van Leeuwen, and Evensen 1998), widely employed in the fields of meteorology (Houtekamer and Mitchell 2005), oceanography (Evensen 1994), and reservoir data assimilation (Aanonsen, Nævdal, Oliver, Reynolds, and Vallès 2009) implicitly estimates the covariance, typically extremely high dimensional due to the spatio-temporal Gaussian random fields involved in

the problems.

The go-to estimator for dependence is the non-parametric sample covariance matrix. This, as is well known, does not necessarily work well in high-dimensional problems and in particular when the number of samples n is smaller than the dimension p where the resulting estimator will be singular. Regularization of the estimation problem is thus necessary. One common method is to use the Moore-Penrose generalized inverse, if a precision estimate is needed, retaining the non-zero eigenvalues of the sample covariance estimate. This is a common method in e.g. filtering methodology and for LDA and QDA. A different school of thought employs Stein-type shrinkage (Stein *et al.* 1956; James and Stein 1961): a convex combination of the sample covariance matrix and some sparse (typically diagonal) target matrix (Ledoit and Wolf 2004). Results for the amount of shrinkage, adaptive to the data, can be found in Ledoit and Wolf (2004); Touloumis (2015), thus computationally costly cross-validation (Stone 1974) might be avoided depending on the target matrix. This method is implemented in the **ShrinkCovMat** R package. For the large class of ensemble filtering algorithms working on random fields, so-called localisation is a necessary tool to overcome the problem of spurious correlations and corresponding noisy update-steps. Two common localisation methods, covariance localisation (Hamill, Whitaker, and Snyder 2001; Houtekamer and Mitchell 2001) and local analysis (Anderson 2003; Evensen 2003; Ott, Hunt, Szunyogh, Zimin, Kostelich, Corazza, Kalnay, Patil, and Yorke 2004; Hunt, Kostelich, and Szunyogh 2007) both work in part on the correlation dependencies from the sample covariance matrix, using kernels to increasingly dampen the strength of dependence as a function of distance between states.

The SPDE approach of Lindgren, Rue, and Lindström (2011) linking the large class of continuous time models having SPDE specifications with the important class of indexed Gaussian Markov random fields (GMRF) (Rue and Held 2005) motivates working directly with the precision matrix instead of the covariance. This in part because of natural modelling assumptions using Markov properties, yielding a more parsimonious model and thus better statistical estimates, but also the computational savings in working with sparse matrices. The sparsity is afforded due to the precision-parametrisation of the multivariate Gaussian with Markov properties. Both the **TMB** and **INLA** packages exploit this sparsity when solving problems involving high dimensional latent variable modelling.

Estimation of sparse precision matrices may be divided into the class of methods that jointly estimates parameters and the Markov properties, and the class that estimates precision conditioned on knowing the zero and non-zero elements of the precision. The former includes methods such as the well known graphical lasso (Friedman, Hastie, and Tibshirani 2008), and column-by-column methods (Yuan 2010; Cai, Liu, and Luo 2011; Zhao and Liu 2014; Liu and Wang 2017). For an overview, see Fan, Liao, and Liu (2016). The latter class of methods typically involves the Gaussian likelihood, see e.g. Hastie *et al.* (2009) or Zhou, Rütimann, Xu, and Bühlmann (2011), which involves iterative optimisation. The method of Le and Zhong (2022) avoids this by utilising a column-by-column method inverting sample covariance matrices of dimension much smaller than the original p . This scheme has both asymptotic results and is also computationally efficient. However, due to working on pure sample-covariance matrices, the numerical scheme may run into problems even for moderate dimensions. Furthermore, the resulting estimate is not symmetric, making e.g. the Cholesky decomposition inadmissible.

GraphSPME combines the precision estimation routine with respect to a graph in Le and Zhong (2022) with the automatic and adaptive shrinkage of sample covariance matrices in

Touloumis (2015), and adds symmetry conversion to obtain computationally stable and fast estimates of precision matrices given some graph or sparsity pattern. The resulting estimates, that are guaranteed to be SPD, are possible to use with efficient factorisation routines such as the Cholesky decomposition when inverting or solving sparse linear systems in general. It also adds methods for estimating the Markov order from data, given a graph of 1'st order neighbours. The package is easy to use, provides fast computation, and works in very high dimensions. Being easily available in C++ as header only, and as Python and R packages under PyPi and CRAN respectively, the package can be integrated in both machine-learning algorithms as well as the large families of ensemble-filtering routines working on dynamical spatio-temporal models.

In Section 2 the ideas and concepts of asymptotic Stein-type shrinkage of the sample covariance estimate are introduced. Section 3 covers in-depth the method of Le and Zhong (2022) that heavily influences this paper. The covariance shrinkage method and the graphical precision method is combined in Section 4 that also introduces methodology for estimating the Markov order of the data. Usage of **GraphSPME** is illustrated through an example in Section 5, while the properties are compared to competing methodologies in Section 6 working on the auto-regressive process where all aspects such as sample size, dimension, and graphical structure of the problem may be controlled and varied. Section 7 concludes and discusses results.

2. High-Dimensional covariance estimation with asymptotic Stein-type shrinkage

It is well known that the sample covariance given by

$$\mathbf{S} = \frac{1}{n-1} \sum_{i=1}^n (\mathbf{x}_i - \bar{\mathbf{x}})(\mathbf{x}_i - \bar{\mathbf{x}})^\top \quad (1)$$

where $\mathbf{x}_i \in \mathbb{R}^{p \times 1}$ are i.i.d random vectors and $\bar{\mathbf{x}}$ the sample mean, is not the best estimator when the number of samples n is smaller than the number of parameters p . In addition to being singular for $n \leq p$, the sample covariance matrix can be poorly conditioned even when $n > p$, which means that inverting it amplifies estimation errors (Ledoit and Wolf 2004). Estimators of covariance are important in many applications and much work has been done to improve them. One promising idea, proposed by Ledoit and Wolf (2004), is to devise estimators based on shrinkage, where the following convex combination of the sample covariance and some target matrix is used as estimator:

$$\mathbf{S}^\star = (1 - \lambda)\mathbf{S} + \lambda\mathbf{T}. \quad (2)$$

Here, \mathbf{T} is a target matrix, for the time being equalling $\nu\mathbf{I}_p$ where \mathbf{I}_p is the $p \times p$ identity matrix and λ and ν are chosen to minimise the risk function $E[\|\mathbf{S}^\star - \Sigma\|_F^2]$ – the expected Frobenius norm on the difference between the population and estimated covariance. We now give a short intuitive introduction to Stein-type shrinkage and how it leads to results used in **GraphSPME**.

Stein *et al.* (1956) showed that the sample mean is inadmissible (there exist better estimators) when $p \geq 3$. James and Stein (1961) proposed a new and better estimator, called the James-Stein estimator, that in essence shrinks individual sample means toward some target. The target is typically, but not necessarily, chosen to be the grand mean or average of averages.

How much each individual sample mean is shrunk is given by a shrinkage factor. To formalise, let $\mathbf{X} \in \mathbb{R}^{n \times p}$ be a matrix of random variables, with sample mean of the j 'th variable equal $\hat{\mu}_j = \frac{1}{n} \sum_{i=1}^n x_{ij}$, and average of averages equal $\tilde{\mu} = \frac{1}{p} \sum_{j=1}^p \hat{\mu}_j$. The James-Stein estimator can then be written as

$$\mu_j^* = (1 - \lambda)\tilde{\mu} + \lambda\hat{\mu}_j \quad (3)$$

which is analogous to Equation 2. The covariance estimator proposed by [Ledoit and Wolf \(2004\)](#) can in similar vein be interpreted as shrinkage towards a grand mean, but now towards $\frac{\text{tr}(\mathbf{S})}{p}$ (average sample variance) instead of the sample mean. Another interesting interpretation as given in [Ledoit and Wolf \(2004\)](#), is that of shrinking the eigenvalues of the sample covariance matrix towards their grand mean.

One issue of the covariance shrinkage estimator (2), is that the optimal shrinkage

$$\lambda = \frac{E[||\mathbf{S} - \boldsymbol{\Sigma}||_F^2]}{E[||\mathbf{S} - \nu\mathbf{I}_p||_F^2]} \quad (4)$$

proposed by [Ledoit and Wolf \(2004\)](#) is not a bona fide estimator, as it depends on the true and unobservable covariance matrix. They solve this by using general asymptotics (where p goes to infinity at the same speed as n) to construct consistent estimators. [Touloumis \(2015\)](#) builds upon this work and is able to derive estimators for λ under a general non-parametric framework. Firstly, it is obtained that

$$\lambda^* = \frac{\text{tr}(\boldsymbol{\Sigma}^2) + \text{tr}^2(\boldsymbol{\Sigma})}{N\text{tr}(\boldsymbol{\Sigma}^2) + \frac{p-N+1}{p}\text{tr}^2(\boldsymbol{\Sigma})}, \quad (5)$$

by first expanding the expectations in the numerator and denominator of (4) and retaining only quantities that are asymptotically non-negligible. To create a consistent estimator of (5), parameter vector the quantities are replaced by consistent estimators constructed using U-statistics. The proposed estimator as given in [Touloumis \(2015\)](#) is

$$\hat{\mathbf{S}}^* = (1 - \hat{\lambda})\mathbf{S} + \hat{\lambda}\hat{\nu}\mathbf{I}_p \quad (6)$$

with

$$\hat{\lambda} = \frac{Y_{2N} + Y_{1N}^2}{NY_{2N} + \frac{p-N+1}{p}Y_{1N}^2} \quad (7)$$

and $\hat{\nu} = Y_{1N}/p$. Y_{1N} and Y_{2N} are constructed using standard results from the theory of U-statistics as $Y_{1N} = U_{1N} - U_{4N}$ and $Y_{2N} = U_{2N} - 2U_{5N} + U_{6N}$.

Similar results follow for alternative target matrices \mathbf{T} and are constructed in the same manner. **GraphSPME** implements the covariance estimator of [Touloumis \(2015\)](#) for a target matrix containing the sample variances on the diagonal. This is available for users, but also employed under-the-hood in precision matrix estimation further elaborated on in Section 4.

3. High-dimensional precision estimation with known Markov properties

The covariance parametrisation of dependence and corresponding estimates of Section 2 are efficient when no more structure on the data generating process is known. However, when e.g. dimensions are known to be conditionally independent, other parametrisations and corresponding estimates may be more efficient. In particular, parametrisations filtering the family of distributions to distributions that factor according to the conditional independence (Bishop and Nasrabadi 2006) are particularly useful. We will here discuss estimation of the precision matrix under Gaussian Markov Random Field assumptions.

Let $\mathcal{G} = (\mathcal{V}, \mathcal{E})$ be a graph with vertices \mathcal{V} and edges \mathcal{E} . A random vector $\mathbf{x} \in \mathbb{R}^d$ is a Gaussian Markov Random Field (GMRF) (Rue and Held 2005) with respect to the graph $\mathcal{G} = (\{1, \dots, d\}, \mathcal{E})$, with mean $\boldsymbol{\mu}$ and symmetric positive definite (SPD) precision matrix Λ if

$$p(\mathbf{x}) = (2\pi)^{-\frac{d}{2}} \sqrt{|\Lambda|} \exp\left(-\frac{1}{2}(\mathbf{x} - \boldsymbol{\mu})^\top \Lambda (\mathbf{x} - \boldsymbol{\mu})\right) \quad (8)$$

and

$$\Lambda_{i,j} \neq 0 \Leftrightarrow (i, j) \in \mathcal{E} \forall i \neq j. \quad (9)$$

One of the advantages of the mean-precision parametrisation versus the mean-covariance parametrisation of the GMRF is the intrinsic filtering of the family of Gaussian distributions. Only the Gaussian distributions satisfying factorisation of the joint distribution due to conditional independence are considered under a known sparsity pattern of the precision. Necessarily, estimation of the precision with known zeroes will imply searching only over distributions that satisfy specified Markov properties corresponding to some pre-specified graph \mathcal{G} . This is, of course, highly beneficial to e.g. spatio-temporal modelling that frequently utilises said properties.

The graphical lasso algorithm (Friedman *et al.* 2008) famously penalises dense precision and searches for an optimal (w.r.t. the Gaussian likelihood) sparsity pattern in the space of SPD matrices. Similar methods estimate the precision column-by-column (Yuan 2010; Cai *et al.* 2011; Zhao and Liu 2014; Liu and Wang 2017) parameter vector by exploiting the relationship between the conditional distributions from the multivariate normal and linear regression to employ lasso-type regression algorithms that enforce sparsity. Common for all these methods is that they search for the sparsity pattern and the corresponding graph, without it being specified pre-estimation.

The problem of estimating the precision matrix under a known sparsity pattern or graphical structure has received less attention than the problem of jointly estimating non-zero and zero elements of the precision as discussed above, and most methods require the Gaussian likelihood (Hastie *et al.* 2009; Zhou *et al.* 2011) in tandem with iterative optimisation. The method of Le and Zhong (2022) is a computationally efficient column-by-column method that explicitly estimates the non-zero elements w_{j1} of column $w_j = \Lambda_{\cdot j}$ of the precision using block-sample covariance matrices. Let \mathbf{B}_j be a matrix of zeroes and ones so that $\mathbf{B}_j w_{j1} = w_j$. Accordingly, let $\mathbf{x}_{i\mathbf{B}_j} = \mathbf{B}_j^\top \mathbf{x}_i$ denote the sub-vector of \mathbf{x}_i where relevant dimensions are "picked-out" by \mathbf{B}_j . Correspondingly, $S_{\mathbf{x},j} = \frac{1}{n-1} \sum_i (\mathbf{x}_{i\mathbf{B}_j} - \overline{\mathbf{x}_{\mathbf{B}_j}})(\mathbf{x}_{i\mathbf{B}_j} - \overline{\mathbf{x}_{\mathbf{B}_j}})^\top$ denotes the j -th block-sample covariance matrix and where $\overline{\mathbf{x}_{\mathbf{B}_j}}$ denotes the sample mean of $\{\mathbf{x}_{i\mathbf{B}_j}\}_{i=1}^n$. Then Le and Zhong (2022) estimates the j -th column-vector of the precision by

$$\hat{w}_j = \mathbf{B}_j S_{\mathbf{x},j}^{-1} \mathbf{B}_j^\top \mathbf{e}_j \quad (10)$$

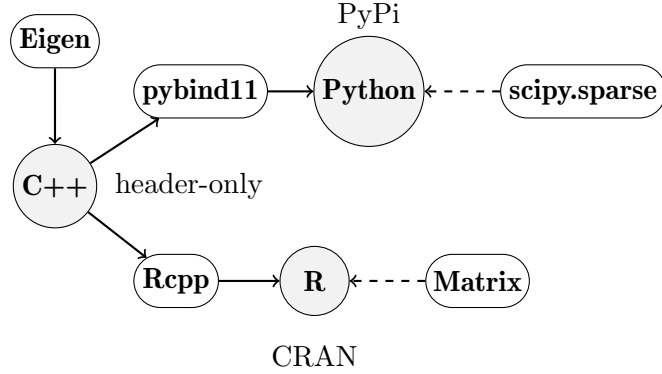


Figure 1: Overview of the **GraphSPME** package. The package is implemented as header-only in C++ (Stroustrup 2000), and exposed to R (R Core Team 2018) (available at CRAN) and Python (Van Rossum and Drake 2009) (available at PyPi) via the packages **Rcpp** (Eddelbuettel and François 2011) and **pybind11** (Jakob *et al.* 2017) respectively. Utilising **GraphSPME** requires sparse matrices, which implementation may be found in e.g. **scipy.sparse** (Virtanen *et al.* 2020) for Python or **Matrix** (Bates *et al.* 2022) for R.

where e_j is the j -th column of the $p \times p$ identity matrix \mathbf{I}_p .

Under relatively mild assumptions of positive bounded eigenvalues of the population covariance and that the $\|\Sigma\|_1$ norm is bounded, Le and Zhong (2022) establishes asymptotic normality on the estimated non-zero elements of column j , \hat{w}_{j1} . The numerical scheme is not guaranteed to succeed, as even a block-sample covariance matrix can be singular, depending on the connectivity of \mathcal{G} and the number of observations n . Furthermore, the estimated precision is generally not symmetric due to the column-by-column nature of the routine. The preceding section seeks to build on the method of Le and Zhong (2022) by targeting these issues, and propose an efficient implementation in the **GraphSPME** library.

4. Software implementation and innovations

At its core, **GraphSPME** implements sparse precision matrix estimation with respect to a known graphical structure as discussed in Section 3. In addition to the method of Le and Zhong (2022), the automatic asymptotic covariance shrinkage estimate of Touloumis (2015) and introduced in Section 2 is also implemented and exposed to users of the package. This allow modifying the sparse precision matrix estimate, to resolve the issue of potential singular block-sample covariance matrices that are repeatedly inverted. It is reasonable to also expect slightly more efficient estimates of the full precision matrix in comparison to the original method that is without any shrinkage. Finally, a symmetry conversion

$$\hat{\mathbf{\Lambda}} = \frac{1}{2} (\tilde{\mathbf{\Lambda}} + \tilde{\mathbf{\Lambda}}^\top) \quad (11)$$

is imposed on the final estimate. This does however not degrade the result: Cai *et al.* (2011) shows that $\hat{\mathbf{\Lambda}}$ achieve the same rate of convergence as $\tilde{\mathbf{\Lambda}}$ asymptotically, and asymptotic results as presented in Le and Zhong (2022) may therefore still be admissible.

4.1. Markov-order estimation

In real applications, the neighbourhood structure is oftentimes known, while the Markov order might be unknown. It may be exactly imposed through modelling choices, such as assuming efficient markets yielding a first order condition on prices, or the modelling assumptions are flexible enough to allow for a structurally-given but specifically unknown dependence structure.

The argument above is the reason for the separation of graphical neighbourhood structure and the Markov order in **GraphSPME**. In the function estimating sparse precision matrices, both the neighbourhood graph (identical to a 1'st order Markov order graph) and the integer Markov order (potentially estimated as above) can be provided as arguments.

For the cases of an unknown Markov order but a given neighbourhood structure, **GraphSPME** implements a function for estimating the exact nature of the order. The underlying method starts at Markov order 0 (independence), iteratively increments the order while running tests, and stops when some ideal order is found. During iterations, the average Gaussian likelihood (and generally the quasi-likelihood)

$$l(\mathbf{\Lambda}) = \frac{1}{2} (\text{tr}(\mathbf{S}\mathbf{\Lambda}) - \log |\mathbf{\Lambda}|) \quad (12)$$

is calculated. This function is monotonically decreasing in Markov order, due to the hierarchical nature of the different models. To decide on some order, penalization must be added. **GraphSPME** utilizes the AIC value, the number of estimated parameters, scaled by n^{-1} as we are working with an average likelihood. (Akaike 1974) Let m be the number of columns in the data \mathbf{X} , and l be the number of non-zero entries in the estimated precision matrix $\hat{\mathbf{\Lambda}}$. The penalized quasi average likelihood is then given as

$$l_{\text{aic}}(\hat{\mathbf{\Lambda}}) = \frac{1}{2} \left(\text{tr}(\mathbf{S}\hat{\mathbf{\Lambda}}) - \log |\hat{\mathbf{\Lambda}}| \right) + \frac{1}{2n}(l + m). \quad (13)$$

Since $\frac{1}{2}(l + m)$ gives the number of parameters due to the symmetry of the precision. The arguments for using the AIC is its computational speed and stability over other information criteria (Takeuchi 1976; Murata, Yoshizawa, and Amari 1994), or computationally costly cross-validation (Stone 1974). In addition, the precision estimating routine employing the block-sample covariance matrices being only a scaling factor away from the maximum likelihood estimate, making the AIC asymptotically amenable.

Note that since datasets typically are finite, it can occur that estimating only a sub-vector of the conceptually true parameter-vector can yield a better result (in expectation on test data) than estimating the full parameter-vector. This is due to the extra variance that is induced by increasing the dimension on the space of parameters. The workflow utilising estimation of Markov order is illustrated in Section 5.

4.2. Implementation details

Figure 1 illustrates the overall structure and dependencies of **GraphSPME**. The core functionality in the package is implemented in C++, relying heavily on the time-tested fast linear-algebra library **Eigen**, and in particular the matrix classes afforded by its sparsity module. It is implemented as header-only, and therefore easily included by other packages. Bindings are also created to both Python and R, for easy availability to users of these languages. For

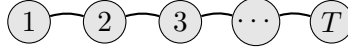


Figure 2: The neighbourhood structure of the mixed-effect AR- p model, corresponding to the graph created for a 1’st order Markov process.

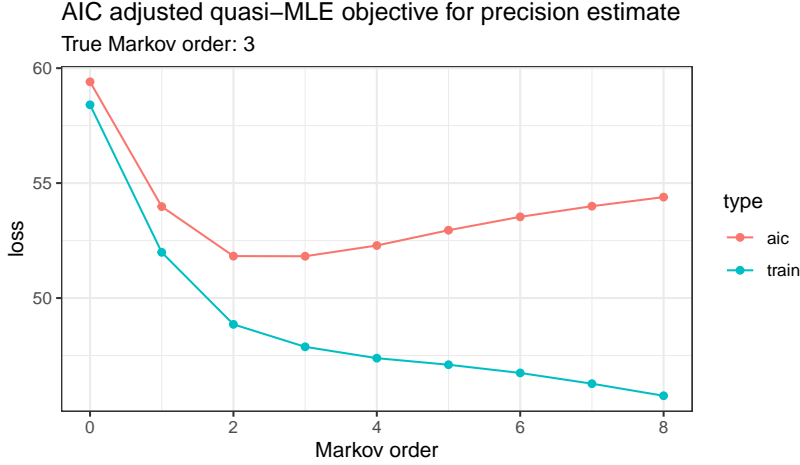


Figure 3: Results from estimating the Markov order for the mixed-effect AR- p model (14). The “train” results are from the average Gaussian loss implemented in `prec_nll`, while the “aic” penalization is obtained through the `prec_aic` implementation. Both taking a precision estimate obtained through the `prec_sparse` function using various degrees of Markov order (x -axis).

Python this is done via `pybind11`, and with `Rcpp` to R. Working with **GraphSPME** in these languages requires libraries making sparse matrices available to represent graphs and return values. For Python, **GraphSPME** is available through PyPi, and through CRAN for R users.

5. Using the GraphSPME package

The goal of **GraphSPME** is to provide dependence estimates with respect to a graph with some degree of connectivity, potentially either fully connected or disconnected. For a fully connected graph, it makes sense to directly estimate the covariance matrix and not the precision matrix. For this edge case (but also very typical), **GraphSPME** provides the `cov_shrink_spd` which returns the shrinkage covariance estimate of [Touloumis \(2015\)](#) for a sample-variance diagonal target matrix presented in Section 2. For all other cases of a not fully connected graph, it is sensible to estimate the precision matrix due to the sparsity afforded by missing vertices between edges relative to the fully connected variant. In such situations, the function `prec_sparse` is implemented, that returns the precision estimate of [Le and Zhong \(2022\)](#) potentially with the shrinkage and symmetry adjustments described in Section 4. `prec_sparse` requires the $n \times p$ dataset as input, along with a graph describing the neighbourhood structure, and an integer Markov order (defaults to 1). If the Markov order is unknown, **GraphSPME** finally implements the AIC for the precision estimate in `prec_aic` for a given training dataset and corresponding precision estimate with some assumed Markov order. This may then be employed to estimate the degree of connectivity in the graph, given a neighbourhood structure.

Following is a walk-through of the above mentioned functions of **GraphSPME**. The full code may be found at https://github.com/equinor/GraphSPME/tree/main/GraphSPME-examples/mixed_effect_arp.R. Consider the i 'th realisation of $i = 1 : n$ -realisations of a random-effect AR- p model

$$x_{i,t} = u_t \sum_{j=1}^p \psi_j x_{i,t-j} + \epsilon_{i,t}, \quad \sum_j \psi_j = 1, \quad u_t \sim U(0,1), \quad \epsilon_{i,t} \sim N(0,1) \quad (14)$$

where the random effects u_t are indexed by time t . Assume that we have a dataset of $n = 100$ independent realisations of this model with final time $T = 100$. For **GraphSPME** it is necessary to work with a defined neighbourhood structure. In this model, the neighbourhood structure correspond to a 1'st order Markov structure as illustrated in Figure 2. To pass this along to `prec_sparse` we create the corresponding sparse matrix G with ones if i is a neighbour of j .

```
R> G <- bandSparse(100, 100,
                  (-1):1,
                  sapply((-1):1, function(j) rep(1,100-abs(j))))
)
```

```
100 x 100 sparse Matrix of class "dgCMatrix"
[1,] 1 1 . . . . .
[2,] 1 1 1 . . . .
[3,] . 1 1 1 . . .
[4,] . . 1 1 1 . .
[5,] . . . 1 1 . .
.....
```

Note that the function `bandSparse` from the **Matrix** package is used to be allowed to work with sparse matrices on the R side, see also Figure 1. In the case when p is unknown, i.e. the Markov order, the user can employ the `prec_aic` function for different precision estimates where the Markov order is incremented through the `markov_order` argument.

```
R> nll <- aic <- numeric(16)
R> for(p in 0:15){
  Prec_est <- prec_sparse(xtr, G, markov_order=p)
  nll[p+1] <- prec_nll(xtr, Prec_est)
  aic[p+1] <- prec_aic(xtr, Prec_est)
}
```

The results are visualised in Figure 3. The routine correctly identifies the AR-3 model, even with relatively little data, making the results very close to the more parsimonious AR-2 model. Given that the Markov-order is identified, the user may produce the final precision estimate through again employing the `prec_sparse` function.

```
R> Prec <- prec_sparse(xtr, G, 3)
```

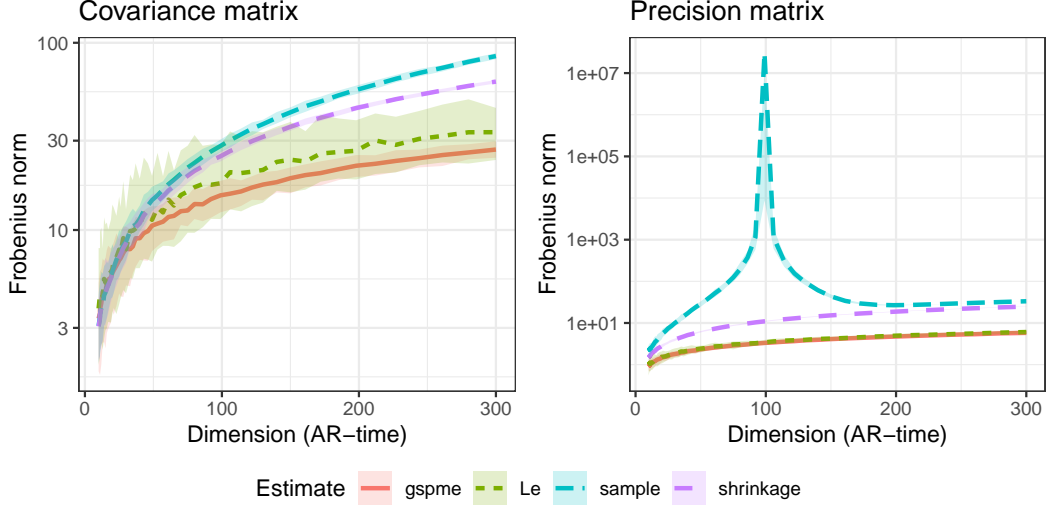


Figure 4: The Frobenius norm (y -axis, log-scale) evaluated on the difference between population covariance (left) or precision (right) matrices and corresponding statistical estimates, explained in the start of Section 6. The statistical process is an AR-1 process with sample size fixed at $n = 100$, and parameter $\psi = 0.8$, while the time or dimension of the problem ranges from 10 to 300 (x -axis). The solid line is the average over 100 Monte Carlo simulations, while the transparent confidence bands yields the empirical 0.05 and 0.95 empirical quantiles.

```
100 x 100 sparse Matrix of class "dgCMatrix"
[1,]  1.2807 -0.4191 -0.1180  0.0653  .      .
[2,] -0.4191  0.9841  0.0659 -0.2544 -0.112  .
[3,] -0.1180  0.0659  1.1742 -0.3586 -0.276  .
[4,]  0.0653 -0.2544 -0.3586  1.1861 -0.319  .
[5,]  .      -0.1123 -0.2765 -0.3190  0.819  .
.....
```

Because the precision estimate is non-parametric, estimates of the fixed effects ψ and the random effects \mathbf{u} may then be found through estimating the conditional expectation of all data-points using the precision estimate

$$E[x_i | x_{ne(i)}] = -\Lambda_{i,i}^{-1} \sum_{j \in ne(i)} \Lambda_{i,j} x_j, \quad (15)$$

which assumes the unconditional mean to be zero, and then relating such estimates to the predictive formula (14) involving both fixed and random effects.

6. High-Dimensional big-data case study

The dependency estimates implemented in **GraphSPME** are tested against one another and also versus the sample covariance matrix as a default benchmark that all estimates should improve upon. To control for uncertainty, we perform 100 Monte Carlo simulations for each experiment. The results are presented visually in figures 4, 5, and 6. Here, the estimate

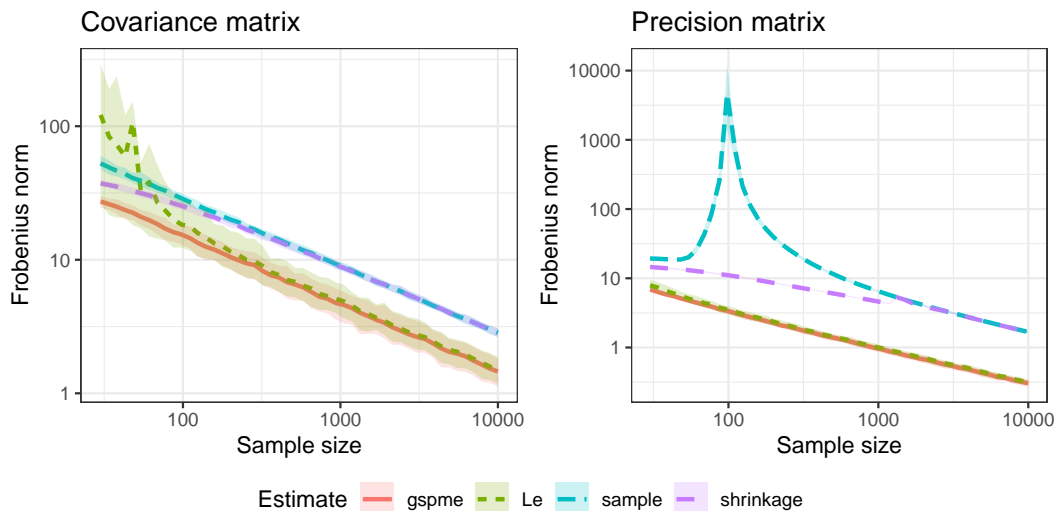


Figure 5: The Frobenius norm (y -axis, log-scale) evaluated on the difference between population covariance (left) or precision (right) matrices and corresponding statistical estimates, explained in the start of Section 6. The statistical process is an AR-1 process with dimension or time fixed at $T = 100$, and parameter $\psi = 0.8$, while the sample size ranges from 30 to 10000 (x -axis, log-scale). The solid line is the average over 100 Monte Carlo simulations, while the transparent confidence bands yields the empirical 0.05 and 0.95 empirical quantiles.

resulting from the estimation routine implemented with **GraphSPME** explained in Section 4 is denoted "gspme", the estimate of [Le and Zhong \(2022\)](#) is denoted "Le", the shrinkage estimate of [Touloumis \(2015\)](#) is denoted "shrinkage", and the benchmark sample covariance estimate (1) is denoted "sample".

We employ the AR- p process having known covariance and precision matrices, so that we may use e.g. the Frobenius norm to measure the accuracy of the estimates. We vary both the sample size, n , the dimension T , and the auto-regressive order p , to test all aspects of the dependence estimates given in **GraphSPME**. As an example, let

$$x_t = \phi x_{t-1} + \epsilon_t, \quad x_1 \sim \mathcal{N}\left(0, \frac{1}{1-\phi^2}\right), \quad \epsilon_t \sim \mathcal{N}(0, 1) \quad (16)$$

be an AR-1 process. Then, the joint distribution of $\mathbf{x} = [x_1, \dots, x_T]^\top$ has dense covariance given by

$$\Sigma = \begin{bmatrix} B(1,1) & \dots & B(1,T) \\ \vdots & \ddots & \vdots \\ B(T,1) & \dots & B(T,T) \end{bmatrix}, \quad \text{where } B(i,j) = \frac{\phi^{|i-j|}}{1-\phi^2}, \quad (17)$$

while the equivalent precision matrix is sparse, and given by

$$\Lambda = \begin{bmatrix} 1 & -\phi & & & \\ -\phi & 1+\phi^2 & -\phi & & \\ & \ddots & \ddots & \ddots & \\ & & -\phi & 1+\phi^2 & -\phi \\ & & & -\phi & 1 \end{bmatrix}. \quad (18)$$

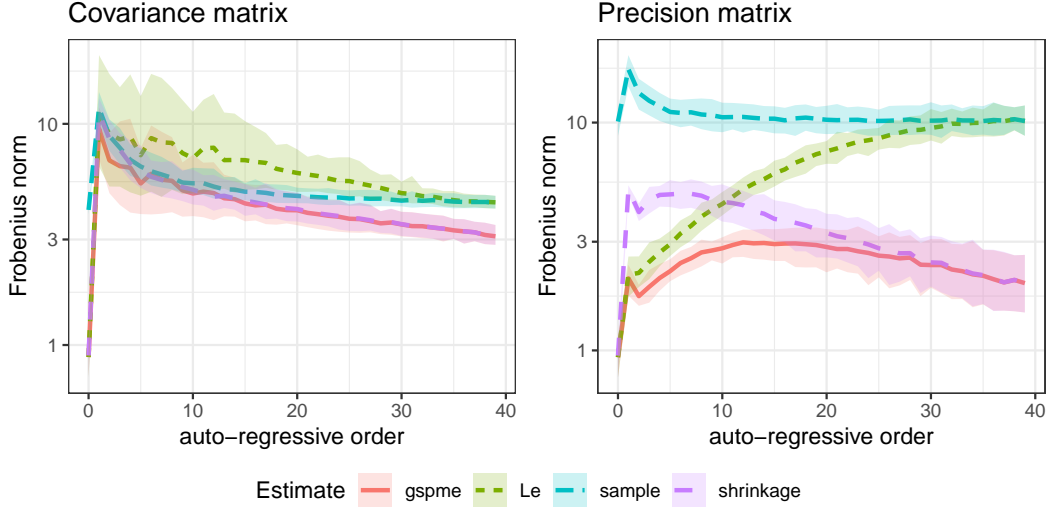


Figure 6: The Frobenius norm (y -axis, log-scale) evaluated on the difference between population covariance (left) or precision (right) matrices and corresponding statistical estimates, explained in the start of Section 6. The statistical process is an AR- p process with sample size fixed at $n = 100$, time fixed to $T = 40$, while the auto-regressive order (p) of the process ranges from 0 (giving independent white noise with a fully disconnected graph) to a fully-connected graph at $p = T - 1 = 39$ (x -axis). All ψ 's are equally set to $0.8/p$. The solid line is the average over 100 Monte Carlo simulations, while the transparent confidence bands yields the empirical 0.05 and 0.95 empirical quantiles.

Similar results hold for the AR- p process - the covariance is dense with elements given by a known autocovariance function, while the precision matrix will be sparse having a band-sparse structure. It is therefore ideally suited to study the properties of dependence estimates with respect to some graph. We use the `ARMA.var` function of the `ts.extend` R-package to calculate the exact population covariance matrix, and then invert it to obtain the population precision matrix. The full code can be found at https://github.com/equinor/GraphSPME/tree/main/GraphSPME-examples/arp_dimension_study.R.

Figure 4 contains the results from fixing sample size $n = 100$ of the AR-1 ($\psi = 0.8$) while varying the dimension of the joint distribution by increasing time $T = 10$ to $T = 300$ and then estimating dependence. Note the log y -axis. Due to the fixed sample size, we expect the difference to the population quantities to be increasing in dimension, as the datapoints take up less and less space in a high-dimensional space (manifesting the curse of dimensionality, as there is decreasing information per unit volume). This is confirmed for all estimation procedures. Both the covariance and the precision figures give the same picture of performance: Looking at the solid lines representing the averages, the **GraphSPME** algorithm dominates the other three, with Le being almost indistinguishable for the precision estimates, but can be seen to vary (having a much broader confidence band) and be much more unstable when inverted to a covariance estimate. This is likely due to the pure block-sample covariance matrices of the method, that are automatically regularised with adaptive shrinkage in **GraphSPME**. The advantage of **GraphSPME** and Le routines over the two covariance estimation routines should come as no surprise, as the population precision is highly sparse with a tre-diagonal

structure. The two graphical precision estimation routines are taking advantage of this. This thus highlights the importance of employing the graphical nature of the problem in high dimensions. The shrinkage method performs overall worse than that of Le, but is seen to be more stable, while dominating the performance of the sample estimate. It also has the benefit of being SPD, and thus has no problems with inversion. The sample estimate on the other hand performs very poorly when a precision estimate is required and when n is close to T , due to becoming more and more singular. This is seen in the figure for the Precision matrix, where the norm spikes at $T = 100 = n$, and then decreases as the generalised Moore-Penrose inverse takes over the inversion.

In Figure 5 all estimates are seen to improve with increased sample size, except for the sample covariance that for a few values of n exhibits the pathological behaviour close to $n = T$ as described above. Once again, the **GraphSPME** algorithm dominates the other three in performance (considering the average from the solid lines). For small sample sizes, the automatic shrinkage afforded by the method of Touloumis (2015), that is implemented in **GraphSPME**, improves the estimates, as compared to the un-regularised variants, i.e., the Le method and sample covariance method. As the sample size is increased, the shrinkage factor is decreased, and necessarily also its effect. Therefore, the method of Le and Zhong (2022) is seen to converge to that of **GraphSPME**, and the sample covariance converges to that of the shrinkage method.

For the experiment presented in Figure 6, the sample size is fixed at $n = 100$ and the time at $T = 40$. The order of the auto-regressive parameter is increased from 0 (specifying Gaussian white noise, a fully disconnected graph, and full independence) to $p = T - 1 = 39$ for a fully connected graph. Firstly, note that the sample covariance estimate is stable and does not change much depending on the auto-regressive order. This is because the sample covariance implicitly always specifies a fully connected graph, and is always maximally flexible. Secondly, we expect to see the performance of the method of Le and Zhong (2022) to converge to that of the sample estimate, while the **GraphSPME** and Touloumis (2015) estimate-performance should intertwine more and more. This behaviour is indeed what can be observed - the method of Le and Zhong (2022) benefits early on from the sparse graph specification, but as the graph becomes fully connected, the method is identical to the implicitly fully connected sample covariance estimate. Similarly, for the **GraphSPME** algorithm, it benefits early on from the sparse precision specification, while for higher values it benefits from the shrinkage afforded by the method of Touloumis (2015). This results in the **GraphSPME** algorithm dominating all others in performance for all values of the auto-regressive order.

7. Discussion

This paper describes **GraphSPME**, a C++ header-only library also available in R and Python as packages for user friendly applications. The package takes advantage of and combines the recent methodology estimating sparse precision matrices with respect to some graphical structure with asymptotic Stein-type shrinkage. Numerical examples showcase the validity results of this combination. The package also implements functions for Markov order estimation. The package can be used for exploratory data analysis, but also as part of machine-learning algorithms, advanced statistical regression algorithms or in the large class of filtering algorithms.

References

- Aanonsen SI, Nævdal G, Oliver DS, Reynolds AC, Vallès B (2009). “The ensemble Kalman filter in reservoir engineering—a review.” *Spe Journal*, **14**(03), 393–412.
- Akaike H (1974). “A new look at the statistical model identification.” *IEEE transactions on automatic control*, **19**(6), 716–723.
- Anderson JL (2003). “A local least squares framework for ensemble filtering.” *Monthly Weather Review*, **131**(4), 634–642.
- Bates D, Maechler M, Jagan M (2022). *Matrix: Sparse and Dense Matrix Classes and Methods*. R package version 1.4-1, URL <https://CRAN.R-project.org/package=Matrix>.
- Bishop CM, Nasrabadi NM (2006). *Pattern recognition and machine learning*, volume 4. Springer.
- Burgers G, Van Leeuwen PJ, Evensen G (1998). “Analysis scheme in the ensemble Kalman filter.” *Monthly weather review*, **126**(6), 1719–1724.
- Cai T, Liu W, Luo X (2011). “A constrained l1 minimization approach to sparse precision matrix estimation.” *Journal of the American Statistical Association*, **106**(494), 594–607.
- Eddelbuettel D, François R (2011). “Rcpp: Seamless R and C++ Integration.” *Journal of Statistical Software*, **40**(8), 1–18. doi:10.18637/jss.v040.i08. URL <http://www.jstatsoft.org/v40/i08/>.
- Evensen G (1994). “Sequential data assimilation with a nonlinear quasi-geostrophic model using Monte Carlo methods to forecast error statistics.” *Journal of Geophysical Research: Oceans*, **99**(C5), 10143–10162.
- Evensen G (2003). “The ensemble Kalman filter: Theoretical formulation and practical implementation.” *Ocean dynamics*, **53**(4), 343–367.
- Fan J, Liao Y, Liu H (2016). “An overview of the estimation of large covariance and precision matrices.” *The Econometrics Journal*, **19**(1), C1–C32.
- Friedman J, Hastie T, Tibshirani R (2008). “Sparse inverse covariance estimation with the graphical lasso.” *Biostatistics*, **9**(3), 432–441.
- Hamill TM, Whitaker JS, Snyder C (2001). “Distance-dependent filtering of background error covariance estimates in an ensemble Kalman filter.” *Monthly Weather Review*, **129**(11), 2776–2790.
- Hastie T, Tibshirani R, Friedman JH, Friedman JH (2009). *The elements of statistical learning: data mining, inference, and prediction*, volume 2. Springer.
- Houtekamer PL, Mitchell HL (2001). “A sequential ensemble Kalman filter for atmospheric data assimilation.” *Monthly Weather Review*, **129**(1), 123–137.

- Houtekamer PL, Mitchell HL (2005). “Ensemble kalman filtering.” *Quarterly Journal of the Royal Meteorological Society: A journal of the atmospheric sciences, applied meteorology and physical oceanography*, **131**(613), 3269–3289.
- Hunt BR, Kostelich EJ, Szunyogh I (2007). “Efficient data assimilation for spatiotemporal chaos: A local ensemble transform Kalman filter.” *Physica D: Nonlinear Phenomena*, **230**(1-2), 112–126.
- Jakob W, Rhineland J, Moldovan D (2017). “pybind11 – Seamless operability between C++11 and Python.” <https://github.com/pybind/pybind11>.
- James W, Stein C (1961). “Proc. Fourth Berkeley Symp. Math. Statist. Probab.” *Estimation with quadratic loss*, **1**, 361–379.
- Kristensen K, Nielsen A, Berg CW, Skaug H, Bell B (2015). “TMB: automatic differentiation and Laplace approximation.” *arXiv preprint arXiv:1509.00660*.
- Le TM, Zhong PS (2022). “High-dimensional precision matrix estimation with a known graphical structure.” *Stat*, **11**(1), e424.
- Ledoit O, Wolf M (2004). “A well-conditioned estimator for large-dimensional covariance matrices.” *Journal of multivariate analysis*, **88**(2), 365–411.
- Lindgren F, Rue H, Lindström J (2011). “An explicit link between Gaussian fields and Gaussian Markov random fields: the stochastic partial differential equation approach.” *Journal of the Royal Statistical Society: Series B (Statistical Methodology)*, **73**(4), 423–498.
- Liu H, Wang L (2017). “Tiger: A tuning-insensitive approach for optimally estimating gaussian graphical models.” *Electronic Journal of Statistics*, **11**(1), 241–294.
- Murata N, Yoshizawa S, Amari Si (1994). “Network Information Criterion-Determining the Number of Hidden Units for an Artificial Neural Network Model.” *IEEE Transactions on Neural Networks*, **5**(6), 865–872.
- Ott E, Hunt BR, Szunyogh I, Zimin AV, Kostelich EJ, Corazza M, Kalnay E, Patil D, Yorke JA (2004). “A local ensemble Kalman filter for atmospheric data assimilation.” *Tellus A: Dynamic Meteorology and Oceanography*, **56**(5), 415–428.
- R Core Team (2018). *R: A Language and Environment for Statistical Computing*. R Foundation for Statistical Computing, Vienna, Austria. URL <https://www.R-project.org/>.
- Rue H, Held L (2005). *Gaussian Markov random fields: theory and applications*. Chapman and Hall/CRC.
- Rue H, Martino S, Chopin N (2009). “Approximate Bayesian inference for latent Gaussian models by using integrated nested Laplace approximations.” *Journal of the royal statistical society: Series b (statistical methodology)*, **71**(2), 319–392.
- Stein C, *et al.* (1956). “Inadmissibility of the usual estimator for the mean of a multivariate normal distribution.” In *Proceedings of the Third Berkeley symposium on mathematical statistics and probability*, volume 1, pp. 197–206.

- Stone M (1974). “Cross-Validatory Choice and Assessment of Statistical Predictions.” *Journal of the Royal Statistical Society. Series B (Methodological)*, pp. 111–147.
- Stroustrup B (2000). *The C++ programming language*. Pearson Education India.
- Takeuchi K (1976). “Distribution of Information Statistics and Validity Criteria of Models.” *Mathematical Science*, **153**, 12–18.
- Touloumis A (2015). “Nonparametric Stein-type shrinkage covariance matrix estimators in high-dimensional settings.” *Computational Statistics & Data Analysis*, **83**, 251–261.
- Van Rossum G, Drake FL (2009). *Python 3 Reference Manual*. CreateSpace, Scotts Valley, CA. ISBN 1441412697.
- Virtanen P, Gommers R, Oliphant TE, Haberland M, Reddy T, Cournapeau D, Burovski E, Peterson P, Weckesser W, Bright J, van der Walt SJ, Brett M, Wilson J, Millman KJ, Mayorov N, Nelson ARJ, Jones E, Kern R, Larson E, Carey CJ, Polat I, Feng Y, Moore EW, VanderPlas J, Laxalde D, Perktold J, Cimrman R, Henriksen I, Quintero EA, Harris CR, Archibald AM, Ribeiro AH, Pedregosa F, van Mulbregt P, SciPy 10 Contributors (2020). “SciPy 1.0: Fundamental Algorithms for Scientific Computing in Python.” *Nature Methods*, **17**, 261–272. doi:10.1038/s41592-019-0686-2.
- Wood SN (2011). “Fast stable restricted maximum likelihood and marginal likelihood estimation of semiparametric generalized linear models.” *Journal of the Royal Statistical Society (B)*, **73**(1), 3–36.
- Yuan M (2010). “High dimensional inverse covariance matrix estimation via linear programming.” *The Journal of Machine Learning Research*, **11**, 2261–2286.
- Zhao T, Liu H (2014). “Calibrated precision matrix estimation for high-dimensional elliptical distributions.” *IEEE transactions on Information Theory*, **60**(12), 7874–7887.
- Zhou S, Rütimann P, Xu M, Bühlmann P (2011). “High-dimensional covariance estimation based on Gaussian graphical models.” *The Journal of Machine Learning Research*, **12**, 2975–3026.

Affiliation:

Berent Ånund Strømnes Lunde
TDI EDT DSD
Equinor
Sandsliveien 90, 5254 Sandsli, Norway
E-mail: berl@equinor.com
Department of Mathematics
Faculty of Mathematics and Natural Sciences
University of Bergen
E-mail: berent.lunde@uib.no

Feda Curic
TDI EDT DSD
Equinor
Sandsliveien 90, 5254 Sandsli, Norway
E-mail: fcur@equinor.com

Sondre Sortland
TDI EDT DSD
Equinor
Sandsliveien 90, 5254 Sandsli, Norway
E-mail: sonso@equinor.com